

High sensitivity optical Faraday-magnetometry with intracavity electromagnetically induced transparency

Qiaolin Zhang¹, Hui Sun^{1,*}, Shuangli Fan¹, and Hong Guo^{2†}

¹*School of Physics and Information Technology, Shaanxi Normal University, Xi'an 710062, China and*

²*State Key Laboratory of Advanced Optical Communication Systems and Networks,*

School of Electronics Engineering and Computer Science,

and Center for Quantum Information Technology, Peking University, Beijing 100871, China

(Dated: May 10, 2016)

We suggest a multiatom cavity quantum electrodynamics system for the weak magnetic field detection based on Faraday rotation with intracavity electromagnetically induced transparency. Our study demonstrates that the collective coupling between the cavity modes and the atomic ensemble can be used to improve the sensitivity. With single probe photon input, the sensitivity is inversely proportional to the number of atoms, and the sensitivity with $0.7(5) \text{ nT}/\sqrt{\text{Hz}}$ could be attained. With multiphoton measurement, our numerical calculations show that the magnetic field sensitivity can be improved to $4.7(9) \text{ fT}/\sqrt{\text{Hz}}$.

PACS numbers: 33.57.+c, 42.50.Pq, 42.50.Gy

I. INTRODUCTION

The ability to detect magnetic field by optical means with high sensitivity [1–3] is a key requirement for a wide range of practical applications ranging from geology and medicine to mineral exploration and defense. A particularly important application is magnetic resonance imaging. A variety of techniques including a superconducting quantum interference device (SQUID) [4], cavity optomechanical [5], negatively charged nitrogen-vacancy (NV) centers in diamond [6, 7], and Bose-Einstein condensate (BEC) [8, 9] have been suggested for extremely high sensitive optical magnetometry. There are two ways for sensing of magnetic fields. One is based on light absorption at a magnetic resonance, for example ⁴He atomic magnetometry by optical pumping [10, 11]. Another way to detect magnetic field is achieved by making use of the changes of the index refraction such as high sensitivity optical magnetometry [12–15] based on electromagnetically induced transparency (EIT) [16, 17].

EIT technique enables one to control the absorption and dispersion, changes the index refractive with cancelled absorption. With the presence of the static magnetic field, the left- and right-circular components of the linear polarized probe field drive different transitions, and thus accumulate different phase shifts. As a result the polarization direction is rotated, which is the so-called Faraday rotation [18]. Large optical Faraday rotation has been observed [19], and has been suggested to detect quantum fluctuation [20], atomic filter [21, 22]. The sensitivity of Faraday rotation to weak magnetic fields naturally suggests it as a magnetometry technique [15, 18].

When an ensemble of two-level atoms is placed inside

an optical cavity, the atom-cavity interaction strength can be enhanced to be $g\sqrt{N}$, where g is the single-atom-cavity coupling strength and N is the number of atoms in the cavity mode. Due to the strong optical confinement and small mode volumes, the optical cavity provide an excellent platform for strong light-matter interactions allowing for vacuum induced transparency [23] and all-optical transistor [24]. The resonator response is consequently drastically modified, resulting in substantial narrowing of spectral features [25–28]. The cavity-enhanced Faraday rotation in NV centers in diamond can push the sensitivity of microwave magnetometer into $\text{aT}/\sqrt{\text{Hz}}$ [7]. Furthermore, owing to the established technology for microcavity fabrication, cavities may be an attractive choice for miniaturized systems.

In the present paper, we suggest a composite atom-cavity system for high sensitivity optical Faraday magnetometry based on intracavity EIT. In doing so, we apply a linear polarized probe field to couple into the cavity, and analyze the transmissions and phase shifts of its left- and right-circular polarized components based on intercavity EIT [25, 29–32]. The main idea is to combine cavity-enhanced Faraday rotation and intracavity EIT. Our study show that the cavity-enhanced Faraday rotation supports the detection of weak magnetic field, and resulting in cavity-enhanced sensitivity. For single probe photon measurement, the sensitivity is inversely proportional to the number of atoms. With multiphoton measurement, the limit of sensitivity can be improved to $4.7(9) \text{ fT}/\sqrt{\text{Hz}}$ from $0.7(5) \text{ nT}/\sqrt{\text{Hz}}$ with single photon measurement. Comparing with the microwave Faraday magnetometry proposed by Xia *et al.* in Ref.[7], the physical mechanism behinds our Faraday magnetometry is intracavity EIT, not the resonance absorption. The transparency peak can therefore be controlled by the driving field and the adjustable number of atoms confined in the cavity. Secondly, our Faraday magnetometry works in the optical wave, instead of microwave.

*hsun@siom.ac.cn

†hongguo@pku.edu.cn

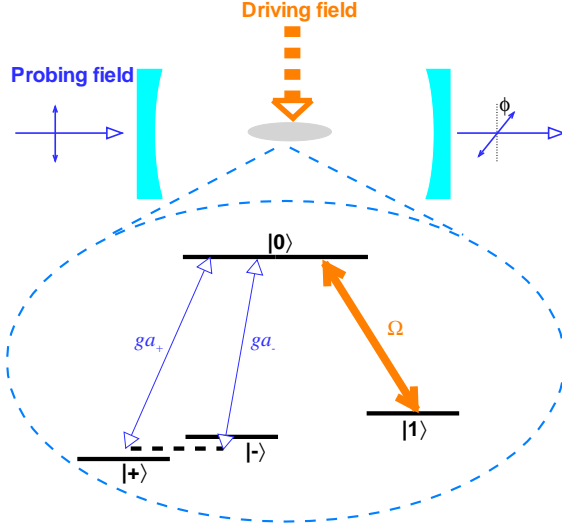


FIG. 1: (Color online) Schematics of setup and atom configuration for weak magnetic field detection. The vertical linear polarized probe field couples into the optical cavity, and then transmits the cavity to the detector. The driving field Ω is free propagating, and it is much larger than the size of the atomic ensemble. We assume the cavity is symmetric such that the loss rates of the cavity fields of the right and left mirrors are equal, i.e., $\kappa_R = \kappa_L = \kappa/2$. The decay rate of the excited state $|0\rangle$ is denoted by 2γ . We assume $g_+ = g_- = g$ for simplicity.

II. SCHEME AND OPTICAL RESPONSES

As depicted in Fig. 1, N identical four-level atoms in tripod configuration, which can be realized in ^{87}Rb D_1 line using hyperfine and Zeeman sublevel of the ground states, are confined in the cavity. The three lower states $|+\rangle$, $|-\rangle$, and $|1\rangle$ correspond to the levels $5^2S_{1/2} |F=1, m_F=+1\rangle$, $|F=1, m_F=-1\rangle$, and $|F=2, m_F=0\rangle$, respectively. We choose the state $5^2P_{1/2} |F=1, m_F=0\rangle$ as the excited state $|0\rangle$. The weak magnetic field lifts the degeneracy of the Zeeman energy level $5^2S_{1/2} |F=1, m_F=\pm 1\rangle$, and the energy shift is denoted by $\delta = g_L \mu_B B$ with g_L and $\mu_B = 14.0 \text{ MHz} \cdot \text{mT}^{-1}$ being Lande g -factor and Bohr magneton. A vertical (V) linear polarized probe field with carrier frequency ω_p couples into the cavity, and its left- and right-circular polarized components (σ_{\pm}) drive the frequency-degenerated left- and right-circular polarized cavity modes ($\{\hat{a}_{\pm}\}$). We denote the detuning between the probe field with the cavity mode by $\Delta = \omega_p - \omega_c$ with ω_c being the cavity mode frequency. The transitions $|\pm\rangle \leftrightarrow |0\rangle$ are driven by the cavity mode $g_{\pm} \hat{a}_{\pm}$. A classical linear polarized driving field with carrier frequency ω_c from free space couples the transition $|1\rangle \leftrightarrow |0\rangle$. Thus the Λ configuration, which is the heart of standard EIT, for cavity modes \hat{a}_{\pm} are formed.

In a rotating frame with the probe and driving field frequencies, the interacting Hamiltonian for the coupled

multiatom-cavity system has the following form

$$H = H_a + H_{af} + H_f, \quad (1)$$

in which

$$H_a = \hbar \sum_i (\Delta_p - \delta) \hat{\sigma}_{++}^i + (\Delta_p + \delta) \hat{\sigma}_{--}^i + \Delta_d \hat{\sigma}_{11}^i, \quad (2a)$$

$$H_{af} = -\hbar \sum_i (g_+ \hat{a}_+ \hat{\sigma}_{0+}^i + g_- \hat{a}_- \hat{\sigma}_{0-}^i + \Omega \hat{\sigma}_{01}^i) + \text{H.c.}, \quad (2b)$$

$$H_f = -\hbar \Delta \hat{a}_+^\dagger \hat{a}_+ - \hbar \Delta \hat{a}_-^\dagger \hat{a}_-, \quad (2c)$$

where $\Delta_p = \omega_p - [\omega_0 - (\omega_+ + \omega_-)/2]$, and $\Delta_d = \omega_d - (\omega_0 - \omega_1)$, are one photon detunings. $\sigma_{\alpha\beta}^i$ ($\alpha, \beta = +, -, 0, 1$) is the atomic operator for the i -th atom. \hat{a}_{\pm} (\hat{a}_{\pm}^\dagger) is the annihilation (creation) operator of the cavity photons, and the cavity-atom coupling coefficient is denoted by $g_{\pm} = \mu_{\pm 0} \sqrt{\omega_c / 2\hbar \epsilon_0 V}$. As usual, we denote the Rabi frequency of the classical driving field by 2Ω . For simplicity, we assume $g_+ = g_- = g$ and the cavity is symmetric, i.e., $\kappa_L = \kappa_R = \kappa/2$.

In the following, we focus our attention on the transmission and the Faraday rotation angle of the probe field. The responses of the two circular polarized components of the probe field can be characterized by intensity transmission coefficients t_{\pm} and the phase shifts ϕ_{\pm} of the corresponding components at the output. Following the standard processes [31, 33], we solve the Heisenberg equations in steady-state and weak-field limit ($g \ll \Omega$). The steady-state solutions read

$$\frac{a_{\pm}^T}{a_{\pm}^{\text{in}}} = t_{\pm} e^{i\phi_{\pm}} = \frac{\kappa}{\kappa - i\Delta - i\chi_{\pm}}, \quad (3)$$

where χ_{\pm} are the atomic susceptibilities, and they are given by

$$\chi_{\pm} = -i \frac{g^2 N}{2(d_{j0} + |\Omega|^2/d_{j1})}, \quad j = +, -, \quad (4)$$

in which $d_{\pm 0} = i(\Delta_p \pm \delta) - \gamma$, $d_{\pm 1} = i(\Delta_p - \Delta_d \pm \delta) - \gamma'$. 2γ is decay rate of the excited state $|0\rangle$, and γ' is the dephasing rate between the three lower states.

In order to provide a detailed picture for weak magnetic field detection, it is illustrative to present the intensity ratio of the cavity transmitted probe fields t_{\pm}^2 and phase shifts ϕ_{\pm} of the two circular components, and they are shown in Figs. 2(a) and 2(b) as functions of the probe detuning Δ_p . We take the relevant parameters as $g\sqrt{N} = 10\gamma$, $\Omega = 1\gamma$, $\Delta_d = \Delta = 0\gamma$, $\kappa = 2\gamma$, $\gamma' = 10^{-3}\gamma$, and $\delta = 10^{-2}\gamma$. As presented in Fig. 2(a), the probe transmissions of the two circular components of probe field are Lorentzian shaped around $\Delta_p = \pm\delta$, and the widths of the transparency peaks are substantially smaller than natural linewidth γ . This is different from the conventional EIT [16, 17]. The weak magnetic field lifts the degeneracy of Zeeman level $|\pm\rangle$, and thus

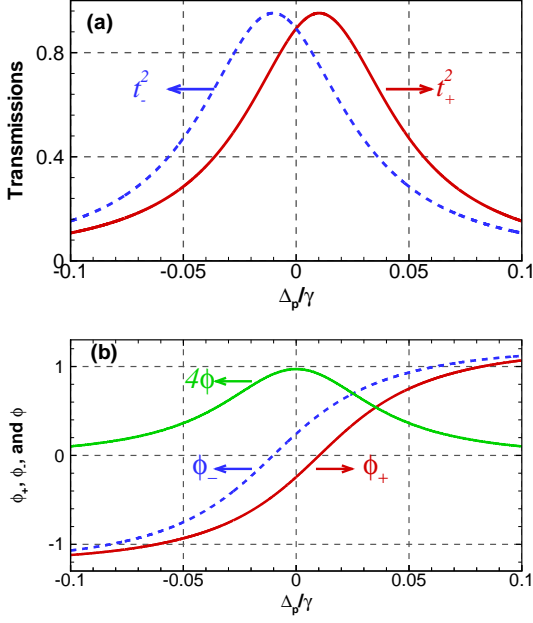


FIG. 2: (Color online) (a) The intensity ratio of the left and right circular polarized cavity-transmitted probe field t_+^2 (solid curve) and t_-^2 (dashed curve) versus the probe detuning Δ_p/γ . (b) The phase shift of the σ_+ and σ_- cavity-transmitted probe field ϕ_+ (solid curve) and ϕ_- (dashed curve) and the Faraday rotation angle ϕ (dotted curve) as functions of the probe detuning Δ_p/γ . The parameters are taken as $g\sqrt{N} = 10\gamma$, $\Omega = 1\gamma$, $\Delta_d = 0\gamma$, $\kappa = 2\gamma$, $\gamma' = 10^{-3}\gamma$, $\Delta = 0$, and $\delta = 10^{-2}\gamma$. The rotation angle ϕ is amplified by four times for clarify.

the positions of the transparency peaks are totally determined by the strength of the magnetic field, i.e., $\Delta_p = \delta$ ($\Delta_p = -\delta$) for σ_+ (σ_-) component. With weak magnetic field presence, we have $t_+^2 = t_-^2 \approx 0.89(6)$. The vanishing absorptions ensure the applications of the composite system for weak magnetic field detection at low-light level.

Within the narrow transparency peaks, the phase shifts of the two components of the probe field ϕ_{\pm} are shown in Fig. 2(b). Owing to intracavity EIT, the dispersion curves are narrowed. As a result, the phase shifts ϕ_+ (solid curve) and ϕ_- (dashed curve) vary rapidly, leading to the enhancement of the Faraday rotation angle $\phi = (\phi_- - \phi_+)/2$. This is the so called cavity-enhanced Faraday rotation [7]. The Faraday rotation angle ϕ versus probe detuning Δ_p is illustrated in Fig. 2(b) with dotted curve. For the sake of clarity, we amplify ϕ by four times. With this set of parameters, the effective half widths of transparency peaks and Faraday rotation angle are, respectively, $w_t \approx 0.04\gamma$ and $\phi \approx 0.26$ rad. Owing to the cavity-enhanced Faraday rotation, the rotation angle ϕ is very sensitive to the magnetic field, which makes the cavity-enhanced sensitivity limit feasible.

In the regime of standard intracavity EIT ($\gamma\gamma' \ll \Omega^2$), and combining with the relation $g\sqrt{N} \gg \Omega$ [17], the effective half widths of the transparency peaks of the two

circular components are [25, 30]

$$w_t \approx \gamma' + 2\kappa \frac{\Omega^2}{g^2 N}. \quad (5)$$

The effective half widths are proportional to $(\Omega/g\sqrt{N})^2$, and they are much smaller than the bare cavity half width 2κ when $g\sqrt{N} \gg \Omega$. We assuming the atomic ensemble is cold, i.e., taking the dephasing rates of the three lower states as $\gamma' = 5 \times 10^{-4}\gamma$ such that the transparent condition $\gamma\gamma' \ll \Omega^2$ can be satisfied [17]. Changing the parameters as $\Omega = 0.5\gamma$ and $g^2 N = 200\gamma^2$, one immediately obtains $w_t \approx 5 \times 10^{-3}\gamma$. The Faraday rotation angle reach $\phi \approx 0.18$ rad with $\delta = 10^{-3}\gamma$. In the typical transparency peaks, the rapid changes in dispersion around two-photon resonance enhance the sensitivity of the Faraday rotation angle on the strength of the weak magnetic field.

In order to see the role of the cavity more clearly, we next calculate the sensitivity to weak magnetic fields, which is the most important characteristic of magnetometry. Applying the resonant conditions ($\Delta_p = \Delta_d = \Delta_c = 0$) and neglecting the dephasing rates ($\gamma' = 0$), we have

$$t_{\pm} = \frac{2\kappa(\delta'^2 + \gamma^2)^{1/2}}{[(2\kappa\gamma - 2\delta\delta' + g^2 N)^2 + 4(\kappa\delta' + \delta\gamma)^2]^{1/2}}, \quad (6)$$

$$\phi_{\pm} = \pm \frac{g^2 N \delta' - 2\delta(\delta'^2 + \gamma^2)}{g^2 N \gamma + 2\kappa(\delta'^2 + \gamma^2)}, \quad (7)$$

in which $\delta' = \delta - \Omega^2/\delta$. At the “resonant point” ($\Delta_p = 0$), the phase shifts of the two circular components of the probe field are exactly equal and opposite in sign due to the symmetry. In the limit of small magnetic field, the polarization rotation angle can be reduced to $\phi = (\phi_- - \phi_+)/2 = \phi_- \simeq (\delta/2\kappa)(g^2 N/\Omega^2)$, which indicates clearly that the Faraday rotation can be enhanced by the collective coupling of atoms with the cavity modes.

III. OPTICAL MAGNETOMETRY AND ITS SENSITIVITY

Assuming the input linear probe field is vertical polarized, the Faraday rotation at the output can be measured by detecting the intensity difference of two linearly polarized components. For each probe, the output has three results: vertical polarized, horizontal polarized, and no photon. The probabilities of three outputs are, respectively, $p(H|\delta) = |t_+ e^{i\phi_+} - t_- e^{i\phi_-}|^2/4$ (H-polarized), $p(V|\delta) = |t_+ e^{i\phi_+} + t_- e^{i\phi_-}|^2/4$ (V-polarized), and $p(0|\delta) = 1 - p(H|\delta) - p(V|\delta)$ (no photon). We show the three outputs as functions of magnetic field induced level shift δ in Fig. 3(a). The probe detuning is taken as $\Delta_p = 0$, and all other relevant parameters are the same as those in Fig. 2. Without the magnetic field, the σ_+ and σ_- components of the probe field experience the same phase shift, and the polarization rotation angle $\phi = 0$. Thus no H-polarized photon can be detected

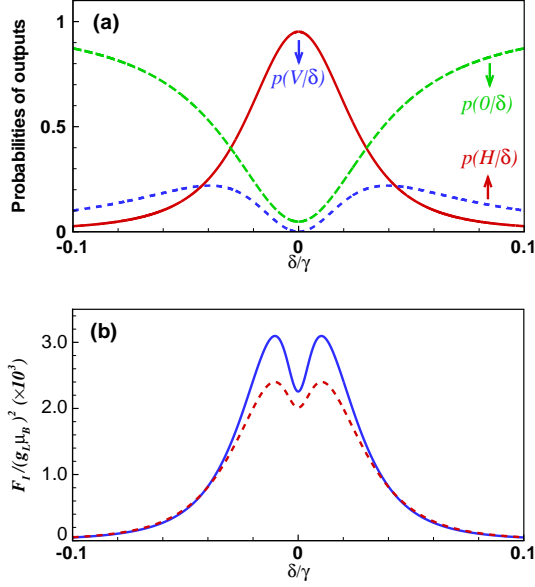


FIG. 3: (Color online) (a) The output probabilities $p(H|\delta)$ (dashed curve), $p(V|\delta)$ (solid curve), and $p(0|\delta)$ (long dashed curve) versus the magnetic field induced level shift δ . (b) Fisher information as a function of δ without (solid curve) and with (dashed curve) Doppler broadening. We take the Doppler width as $\Delta\omega_D \simeq 0.56$ MHz (corresponding to $T = 1$ mK). The relevant parameters are taken as $\Delta_p = \Delta_d = 0$, and other parameters are same as those in Fig. 2.

[see the dashed curve in Fig. 3(a)]. With increasing of the magnetic field, $p(H|\delta)$ increases, and reaches its maximum value $p(H|\delta)_{\max} = 0.27(2)$ at $\delta = \pm 0.042(5)\gamma$. Increasing δ much more, no transmitted photons can be detected.

The parameter δ can be estimated from the outputs. The maximum information about weak magnetic field that can be extracted from the measurement is given by the Fisher information [34], which determines the limit of the sensitivity. With single photon measurement, we have [35]

$$S \geq \frac{1}{\sqrt{\varsigma F(\delta)}}, \quad (8)$$

where ς is the number of times the procedure is repeated, and the Fisher information $F(\delta)$ is given by

$$F(\delta) = (g_L \mu_B)^2 \sum_{x=H,V,0} \frac{1}{p(x|\delta)} \left[\frac{\partial p(x|\delta)}{\partial \delta} \right]^2. \quad (9)$$

In practice, the atoms may move with velocity v , giving the $1/e$ temperature related Doppler width of the atomic ensemble as $\Delta\omega_D = \sqrt{2k_B T \omega^2 / (mc^2)}$ [27]. With $T = 1.0$ mK, we immediately have $\Delta\omega_D \simeq 0.56$ MHz. Considering the influence of Doppler broadening, the Fisher information can be rewritten as

$$F(\delta) = \frac{1}{\sqrt{\pi \Delta\omega_D^2}} \int_{-\infty}^{\infty} F(\delta, kv) e^{-(kv)^2 / \Delta\omega_D^2} d(kv), \quad (10)$$

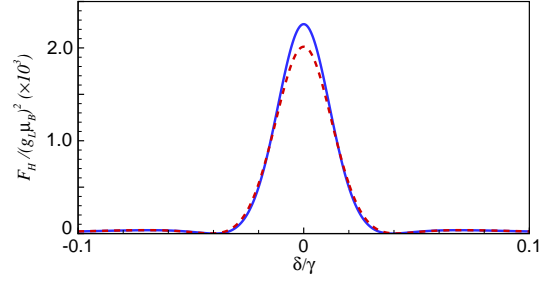


FIG. 4: (Color online) Fisher information of the horizontal polarized output as a function of δ without (solid curve) and with (dashed curve) Doppler broadening. All parameters are same as those in Fig. 3(b).

in which k is wave vector of the probe field. The Fisher informations without (solid curve) and with (dashed curve) Doppler broadening versus level shift δ are depicted in Fig. 3(b). All parameters are the same as those in Fig. 3(a). Confining the atomic ensemble in optical cavity, the detuning between the cavity mode and the probe field accrues an extra phase. While owing to the symmetry of the atomic configuration under consideration, we ignore the systematic errors associated with ac Stark shifts [14]. In the regime considered previously ($g\sqrt{N} \gg \Omega$), Equation (3) shows that the influence of the cavity shift on Fisher information can be safely neglected. With the realistic experimental parameters ($^{87}\text{Rb } D_1$ line), $\hbar\omega_p = 1.55(9)\text{eV}$, $\gamma = \pi \times 6.06$ MHz, $\gamma' = 10^{-3}\gamma = \pi \times 6.06$ kHz, $g^2 N = 100\gamma^2$, $\Omega = 1\gamma$, $\kappa = 2\gamma$, the sensitivity can be calculated to be $2.3(1)\text{nT}/\sqrt{\text{Hz}}$.

Recalling the limit of small magnetic fields, and combining the relation $g\sqrt{N} \gg \Omega$, the Fisher information $F(\delta)$ can be expanded as

$$F(\delta) \simeq (g_L \mu_B)^2 \left[\frac{2}{\kappa^2} \left(\frac{g\sqrt{N}}{\Omega} \right)^4 + \mathcal{O}(\delta^2) \right]. \quad (11)$$

The first dominating term demonstrates that the Fisher information is proportional to $g^2 N / \Omega^2$. Recalling the relation (8), one immediately obtains $S \sim 1/N$, which indicates that the sensitivity is inversely proportional to the number of atoms confined in the cavity. This is the main result of the collective coupling between the cavity modes and atomic ensemble. It is therefore feasible to improve the sensitivity by increasing the value of $g^2 N / \Omega^2$. Taking $g^2 N = 200\gamma^2$ and $\Omega = 0.5\gamma$, the sensitivity can be improved to $0.7(5)\text{nT}/\sqrt{\text{Hz}}$ with single photon measurement. It should be noted that a rise in atomic density is accompanied by an increasing in dephasing rates between metastable lower levels in such a system, and therefore optimal operating conditions have to be carefully matched.

For multi photon measurement, following the processes [7], the limit of the sensitivity can be estimated

by

$$S \geq \frac{t}{\sqrt{F_H}} \sqrt{\frac{\hbar\omega_p \sin^2 \phi + 2K_B T}{P_{\text{in}}}}, \quad (12)$$

in which $F_H = (g_L \mu_B)^2 [\partial_\delta^2 p(H|\delta)]^2 / p(H|\delta)$ is the normal Fisher information of the horizontal polarized output, and K_B is the Boltzmann constant, P_{in} denotes the input probe power. In the above derivation, the noise due to the internal loss channels are included. Equation (12) indicates that the sensitivity is inversely proportional to $\sqrt{P_{\text{in}}}$, and thus can be improved by increasing the probe power. The normal Fisher information of the horizontal polarized output is given by

$$F_H = \frac{1}{\sqrt{\pi \Delta\omega_D^2}} \int_{-\infty}^{\infty} F_H(kv) e^{-(kv)^2 / \Delta\omega_D^2} d(kv). \quad (13)$$

The evolution of F_H versus δ with (dashed curve) and without (solid curve) Doppler broadening are shown in Fig. 4. All parameters are the same as those in Fig. 3(b). One obtains $F_H \simeq 2000(g_L \mu_B)^2 \text{ T}^{-2}$ (with Doppler broadening). With $P_{\text{in}} = 1 \text{ mW}$, $T = 1 \text{ mK}$, the sensitivity can be immediately calculated to be $16.7(8) \text{ fT}/\sqrt{\text{Hz}}$ with $g^2 N = 100\gamma^2$ and $\Omega = 1.0\gamma$. Changing the set of parameters as $g^2 N = 200\gamma^2$ and $\Omega = 0.5\gamma$, numerical calculations show that the sensitivity with $4.7(9) \text{ fT}/\sqrt{\text{Hz}}$ can be achieved with high transmission [$t_+^2 = t_-^2 \simeq 0.76(3)$].

IV. CONCLUSIONS

We have analyzed the cavity-enhanced optical Faraday rotation for weak magnetic field detection in a cavity QED system consisting of four-level atomic ensemble in tripod configuration confined in cavity based on intra-cavity EIT. Owing to the collective coupling between the cavity modes and atomic ensemble, the Faraday rotation can be enhanced dramatically, and therefore leading to cavity-enhanced sensitivity. With single photon measurement, the sensitivity is inversely proportional to the number of the atoms, and our numerical calculations show that the sensitivity with $0.7(5) \text{ nT}/\sqrt{\text{Hz}}$ can be achieved. While the sensitivity can be improved by increasing the probe power with multiphoton measurement, and sensitivity with $4.7(9) \text{ fT}/\sqrt{\text{Hz}}$ could be attained. The cavity-enhanced Faraday rotation can be of interest in atomic filter and quantum information processing.

ACKNOWLEDGMENT

We would like to acknowledge useful discussion with Gongwei Lin. This work was supported by the NSF Shaanxi Province (2014JM2-1001), as well as the Central University (GK201505034).

-
- [1] D. Budker and M. Romalis, *Nature Phys.* **3**, 227 (2007).
 - [2] A. Edelstein, *J. Phys.: Condens. Matter* **19**, 165217 (2007).
 - [3] J. M. Taylor, P. Cappellaro, L. Childress, L. Jiang, D. Budker, P. R. Hemmer, A. Yacoby, R. Walsworth, and M. D. Lukin, *Nat. Phys.* **4**, 810 (2008).
 - [4] M. V. Romalis and H. B. Dang, *Mater. Today* **14**, 258 (2011).
 - [5] S. Forstner, S. Prams, J. Knittel, E. D. van Ooijen, J. D. Swaim, G. I. Harris, A. Szorkovszky, W. P. Bowen, and H. Rubinsztein-Dunlop, *Phys. Rev. Lett.* **108**, 120801 (2012).
 - [6] K. Jensen, N. Leefer, A. Jarmola, Y. Dumeige, V. M. Acosta, P. Kehayias, B. Patton, and D. Budker, *Phys. Rev. Lett.* **112**, 160802 (2014).
 - [7] Keyu Xia, Nan Zhao, and J. Twamley, *Phys. Rev. A* **92**, 043409 (2015).
 - [8] Y. Eto, H. Ikeda, H. Suzuki, S. Hasegawa, Y. Tomiyama, S. Sekine, *Phys. Rev. A* **88**, 031602(R) (2013).
 - [9] W. Muessel, H. Strobel, D. Linnemann, D. B. Hume, and M. K. Oberthaler, *Phys. Rev. Lett.* **113**, 103004 (2014).
 - [10] D. D. McGregor, *Rev. Sci. Instrum.* **58**, 1067 (1987).
 - [11] T. Wu, X. Peng, Z. Lin, and H. Guo, *Rev. Sci. Instrum.* **86**, 103105 (2015).
 - [12] M. O. Scully and M. Fleischhauer, *Phys. Rev. Lett.* **69**, 1360 (1992).
 - [13] M. Fleischhauer and M. O. Scully, *Phys. Rev. A* **49**, 1973 (1994).
 - [14] M. Fleischhauer, A. B. Motsko, and M. O. Scully, *Phys. Rev. A* **62**, 013808 (2000).
 - [15] D. Petrosyan and Y. P. Malakyan, *Phys. Rev. A* **70**, 023822 (2004).
 - [16] J. P. Marangos, *J. Mod. Opt.* **45**, 471 (1998).
 - [17] M. Fleischhauer, A. Imamoglu, and J. P. Marangos, *Rev. Mod. Phys.* **77**, 633 (2005).
 - [18] D. Budker, W. Gawlik, D. F. Kimball, S. M. Rochester, V. V. Yashchuk, and A. Weis, *Rev. Mod. Phys.* **74**, 1153 (2002).
 - [19] M. Atature, J. Dreiser, A. Badolato, and A. Imamoglu, *Nat. Phys.* **3**, 101 (2007).
 - [20] S. W. Chen and R. B. Liu, *Sci. Rep.* **4**, 4695 (2014).
 - [21] Z. M. Tao, Y. L. Hong, B. Luo, J. B. Chen, and H. Guo, *Opt. Lett.* **40**, 4348 (2015).
 - [22] L. F. Yin, B. Luo, A. H. Dang, and H. Guo, *Opt. Express* **22**, 7416 (2014).
 - [23] H. Tanji-Suzuki, Wenlan Chen, R. Landig, J. Simon, and V. Vuletić, *Science* **333**, 1266 (2011).
 - [24] Wenlan Chen, K. M. Beck, Robert Bücker, M. Gullans, M. D. Lukin, H. Tanji-Suzuki, and V. Vuletić, *Science* **341**, 768 (2013).
 - [25] M. D. Lukin, M. Fleischhauer, M. O. Scully, and V. L. Velichansky, *Opt. Lett.* **23**, 295 (1998).
 - [26] H. B. Wu, J. Gea-Banacloche, and M. Xiao, *Phys. Rev. Lett.* **100**, 173602 (2008).
 - [27] J. Gea-Banacloche, H. B. Wu, and M. Xiao, *Phys. Rev. A* **78**, 023828 (2008).

- [28] Y. D. Peng, A. H. Yang, D. H. Li, H. G. Zhang, Y. P. Niu, and S. Q. Gong, *Laser Phys. Lett.* **11**, 065201 (2014).
- [29] M. Albert, A. Dantan, and M. Drewsen, *Nature Photon.* **5**, 633 (2011).
- [30] A. Dantan, M. Albert, and M. Drewsen, *Phys. Rev. A* **85**, 013840 (2012).
- [31] Bichen Zou and Yifu Zhu, *Phys. Rev. A* **87**, 053802, (2013).
- [32] A. Sharma, T. Ray, R. V. Sawant, G. Sheikholeslami, S. A. Rangwala, and D. Budker, *Phys. Rev. A* **91**, 043824 (2015).
- [33] D. F. Walls and G. J. Milburn, *Quantum Optics* (Springer-Verlag, Berlin, Heidelberg, 1994).
- [34] M. Zwiernz, C. A. Pérez-Delgado, and P. Kok, *Phys. Rev. Lett.* **105** 180402 (2010).
- [35] S. L. Braunstein and C. M. Caves, *Phys. Rev. Lett.* **72**, 3439 (1994).